# The Effect of Gurney Flap and Trailing-edge Wedge on the Aerodynamic Behavior of an Axial Turbine Blade

Mohammad Mahdi Mahzoon [1], Masoud Kharati-Koopaee [1*]

[1] Department of Mechanical and Aerospace Engineering, Shiraz University of Technology, Shiraz, Iran.

## Abstract

In this research, the effect of Gurney flap and trailing-edge wedge on the aerodynamic behavior of blunt trailing-edge airfoil Du97-W-300, which is equipped with a vortex generator is studied. To do this, the role of Gurney flap and trailing-edge wedge on the lift and drag coefficient and also aerodynamic performance of the airfoil is studied. Validation of the numerical model is done by comparing the results of the model to the results of the experiment. Results show that before stall, the Gurney flap leads to an increase in the aerodynamic performance in a wider range of angle of attack. Numerical findings reveal that the maximum increment in aerodynamic performance is obtained at a low angle of attack when a trailing-edge wedge is employed. It is found that for the highest considered values of Gurney flap and trailing-edge wedge heights, where the highest values for the lift occur, the higher aerodynamic performance at low angle of attack is obtained when a trailing-edge wedge is used, and at high angle of attack, the Gurney flap results in higher aerodynamic performance. It is also shown that when high aerodynamic performance is concerned, addition of Gurney flap to the airfoil leads to the higher value for the lift.

*Keywords:* Gurney Flap; Trailing-edge Wedge; Wind Energy; Aerodynamic Performance; Axial Turbine.

## 1. Introduction

Thick airfoils are common in wind turbines as they are subjected to relatively high loads in operation. The most significant issue associated to the thick airfoils is the drag penalty due to flow separation especially at high angles of attack. To overcome this difficulty, Vortex Generators (VGs), which was first introduced by Taylor [1], could be used to mitigate the separation region on the airfoil surface and so increase the airfoils aerodynamic behavior [2-4]. In this context, some devices such as the Gurney flap or trailing-edge wedge have also received attention by researchers, as these devices could enhance the aerodynamic behavior of the airfoils [5].

There are several works in the literature focused on the effect of VGs on the aerodynamic behavior of airfoils. Mueller-Vahl et al. [6] investigated the effects of VGs' size, spanwise spacing, and also chordwise position of VGs on the aerodynamic behavior. They found that a decrease in the adjacent VGs led to an increase in the static stall angle and the maximum obtained lift. In their research, they also obtained the optimum chordwise position of the VGs. Velte and Hansen [7] conducted experimental research to study the flow behind VGs on a DU 91-W2-250 airfoil near the stall. It was shown that the existence of VGs resulted in a much less separated boundary layer, and on average, the employment of VGs caused an attached flow on the airfoil surface. Zhao et al. [8] proposed a parameterized VGs array model for the VGs in a counter rotating arrangement on a wing. In this research, they investigated the inter-effects between arrays and estimated the maximum generated circulation of the wings. Prince et al. [9] performed a research to examine the effect

of air jet VGs on the performance of a wind turbine. They showed that VGs could suppress the trailing edge separation onset and enhance the maximum output power, while decreasing the sensitivity to the unsteadiness, which may occur in the wind speed. Suarez et al. [10] focused on the impact of rod VG on the blade of a horizontal axis wind turbine. They indicated that this device could reattach the flow to the blade and enhance the aerodynamic behavior of the turbine. They also showed that the rod VG could prevent penetration of separation toward the blade tip. Zhu et al. [11] conducted a study to examine the effect of single-row and double-row VGs on the dynamic stall of a wind turbine airfoil. Their research revealed that the considered VGs could delay the dynamic stall onset and increase the maximum lift coefficient of the airfoil. They also indicated that the double-row VGs resulted in more suppression of the flow separation than the single-row ones.

Some studies have been conducted to examine the effect of Gurney flap or trailing-edge wedge on the aerodynamics of the airfoils. Nikoueeyan et al. [12] studied the aerodynamic coefficients of a wind turbine airfoil in the presence of Gurney flap. They found that the static lift and moment coefficients were similar to those of the dynamic pitching case where the attached flow regime occurred. Twele and Weinzierl [13] conducted a parametric study of Gurney flaps for wind turbine blades. In this work, they found that improvement in aerodynamic behavior could be attained when relatively small Gurney flap heights at specific blade positions were employed. Zhang et al. [14] investigated the impact of Gurney flap at the inboard part of the blade. Their work revealed that this deployment could effectively enhance the power coefficient of the blade. Gao et al. [15] performed a research to study the effect of trailing-edge wedge on the aerodynamic behavior of an airfoil which was equipped with VGs. Their study showed that the employment of both devices led to better performance than separate devices. Yan et al. [16] compared the effects of Gurney flap and also trailing-edge wedge on the aerodynamic of an airfoil. They indicated that at a certain Gurney flap and trailing-edge wedge height, the trailing-edge wedge could results in a better performance than the Gurney flap.

Exploring the above mentioned works, one could see that although the effect of VGs, Gurney flap or trailing-edge wedge have been examined in some researches, however, the impacts of Gurney flap and trailing-edge wedge on the aerodynamic behavior of the airfoils equipped with VGs have not been studied yet, which is the motivation for the present work. The objective of the current work is to illustrate the change in the lift coefficient, drag coefficient and aerodynamic performance (i.e., lift to drag ratio) of an airfoil equipped with VGs in the presence of Gurney flap and trailing-edge wedge. For this purpose, the blunt trailing-edge airfoil Du97-W-300 is considered for numerical calculation and results are obtained and discussed at different angles of attack and various heights of Gurney flap and trailing-edge wedge.

## 2. Problem Description

In the current work, as mentioned earlier, a blunt trailing-edge airfoil Du97-W-300 which is equipped with VG is considered for numerical calculations. The considered airfoil has a chord length of $c$=0.6 m [17], maximum thickness to chord ratio of $\kappa$=30% [17] and width of $w$=70 mm. The concerned airfoil has a thick trailing edge with thickness of 1.74% of the chord length [17]. The considered airfoil is equipped with VGs in counter-rotational configuration. In counter-rotational configuration, the adjacent VGs have a same incident angle to the flow but opposite. Exploring literature reveals that this configuration has a good potential in suppression of flow separation [18, 19]. The VGs are located at the distance of 20% of the chord length from the leading edge, as this location could lead to a best performance [6]. Figure 1 represents the considered blunt trailing-edge airfoil Du97-W-300 equipped with two pairs of counter-rotational VGs.
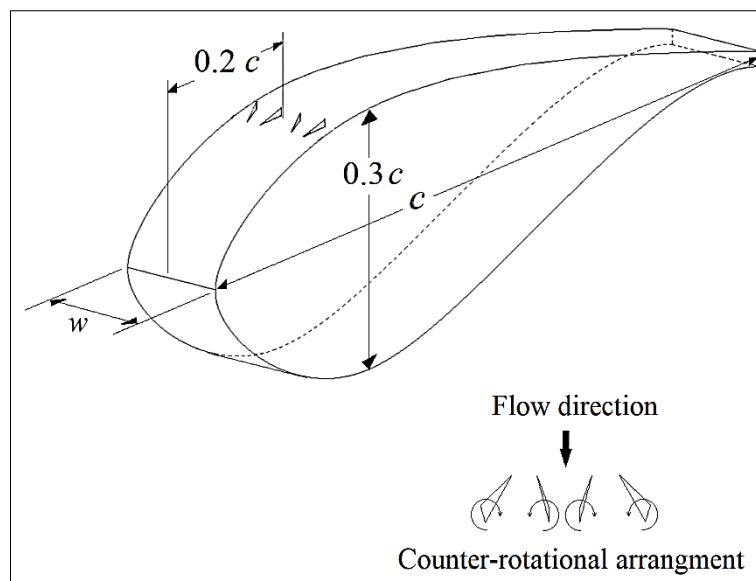


**Figure 1. Blunt trailing-edge airfoil Du97-W-300 equipped with two pairs of counter-rotational VGs**

Figure 2 depicts the geometric parameters of the VGs. The considered geometric parameters could lead to a good aerodynamics behavior of the airfoil [17].
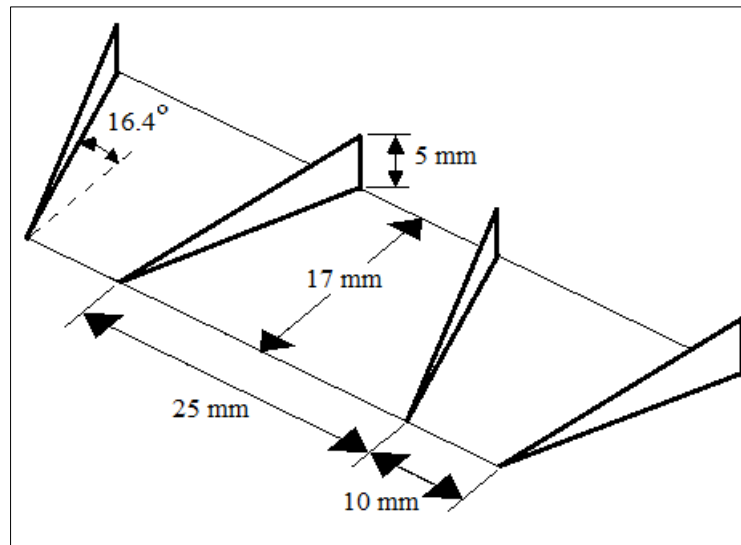
**Figure 2. The geometric parameters of the considered VGs**

In the current work, the Gurney flaps and wedges are attached to the airfoil at the trailing edge. Three different height to the airfoil chord ratios of $H/c=0.5$, 1 and 2% are considered for the Gurney flap and trailing-edge wedge. The length of trailing-edge wedges along the airfoil chord are also considered to be $l/c=2\%$ of the airfoil chord. Figure 3 represents the geometric parameters of the considered Gurney flaps and trailing-edge wedges.
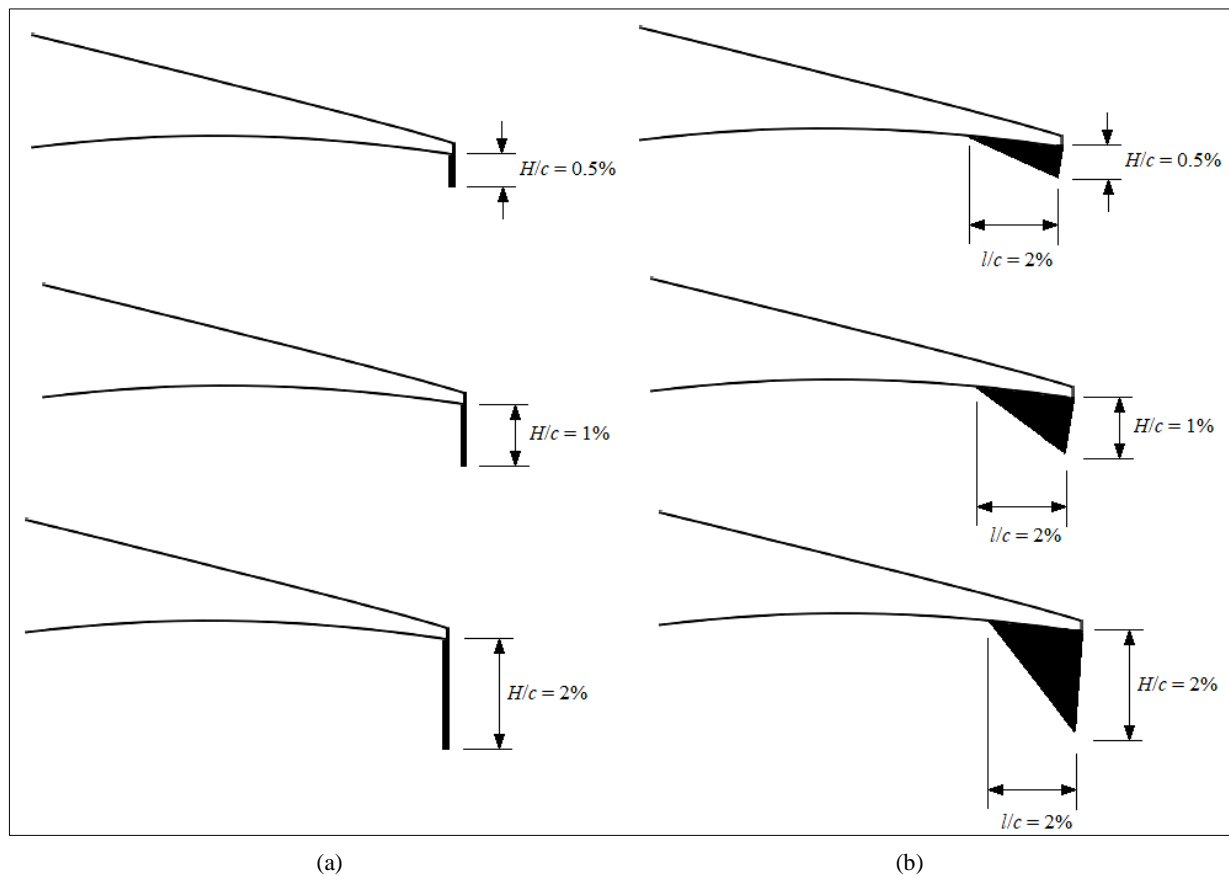
(a)　　　　　　　　　　　　　　　　　　　　　　　　(b)

**Figure 3. Geometric parameters of the considered (a) Gurney flaps and (b) trailing-edge wedges**

To assess the effect of Gurney flap and tailing-edge wedge on the aerodynamics behavior of the airfoil equipped with VGs, lift coefficient ($C_L$), drag coefficient ($C_D$) and also aerodynamic performance of the airfoil ($C_L/C_D$) are obtained and compared. Lift and drag coefficients are defined as the followings:

$$C_L = \frac{L}{\frac{1}{2}\rho V^2 cw} \tag{1}$$

$$C_D = \frac{D}{\frac{1}{2}\rho V^2 cw} \tag{2}$$

where $L$ and $D$ are lift and drag forces of the airfoil and $\rho$ and $V$ are air density and free stream air velocity, respectively. In the present work, results are obtained at angle of attack range of $\alpha=5°$-$20°$. Flow Reynolds number is also considered to be $R_e=\rho Vc/\mu=3\times10^6$ (where $\mu$ stands for the air viscosity), which is in the operating Reynolds number of the wind turbines [5].

## 3. Numerical Procedure

In order to investigate how Gurney flap and trailing-edge wedge affect the aerodynamics behavior, a steady 3-D analysis is performed. The flow is assumed to be incompressible and turbulent with constant properties. Simulation of turbulent flow around the airfoil is accomplished using Spalart-Allmaras turbulence as this model leads to results with appropriate accuracy in 3-D flow around turbine blades [20, 21]. Thus, the governing equations would be the steady incompressible form of the continuity and momentum equations along with the Spalart-Allmaras turbulence model. Numerical calculation is carried out using finite volume technique utilizing the commercial computational fluid dynamics software, ANSYS Fluent.

Figure 4 shows the computational domain used for numerical simulations. The velocity is set for surface $A$ and surface $B$ is set as pressure outlet. Surfaces $C$ and $D$ are set as symmetry. The distances of airfoil from the front and rear of the computational domain are chosen to be 10 and 20 times of the airfoil chord, respectively. The domain size study shows further increase in the domain size has no effect on the results. The no slip condition is imposed on the airfoil, vortex generators, Gurney flap and trailing-edge wedge surfaces.
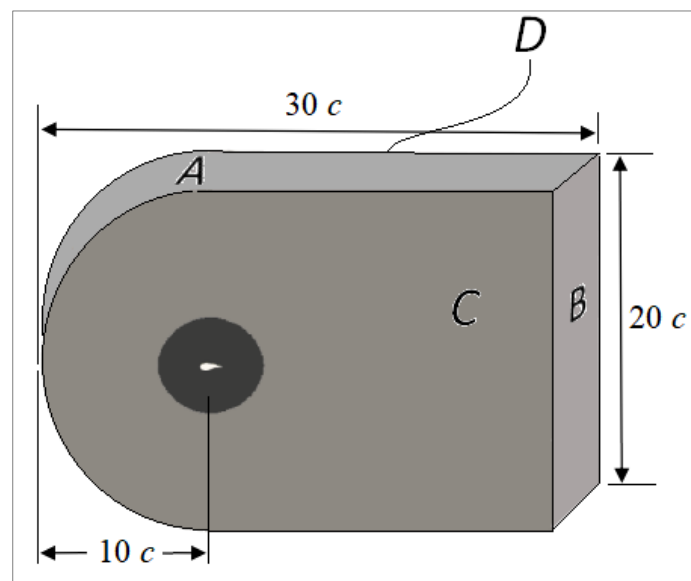


**Figure 4. Computational domain used for numerical simulations**

In this research, second order upwind scheme is utilized for discretization of the governing equations and SIMPLE algorithm is implemented for the pressure-velocity coupling. Residuals are also considered as the convergence criterion and iteration is stopped as they reach less than around $10^{-5}$.

## 4. Grid Study and Validation

The mesh is generated using ANSYS Meshing. Unstructured gird topology is used in the vortex generators region and structured grid topology is generated near the airfoil surface. Figure 5 depicts the generated grid for the whole domain. Figure 6 also presents near field pictures of the grid in the regions of vortex generators, Gurney flap and trailing-edge wedge.
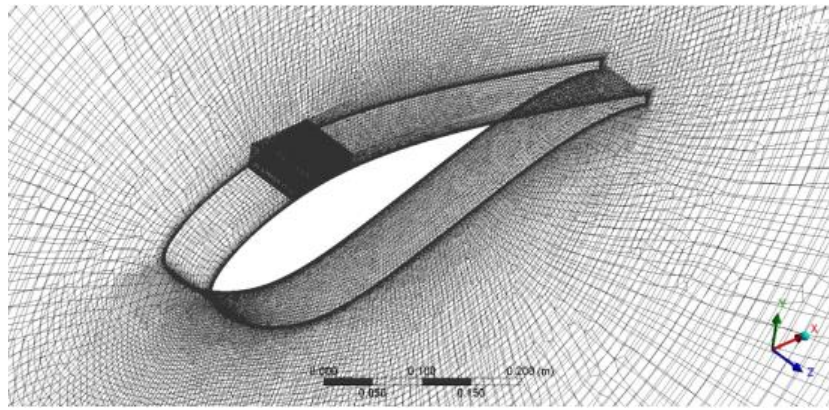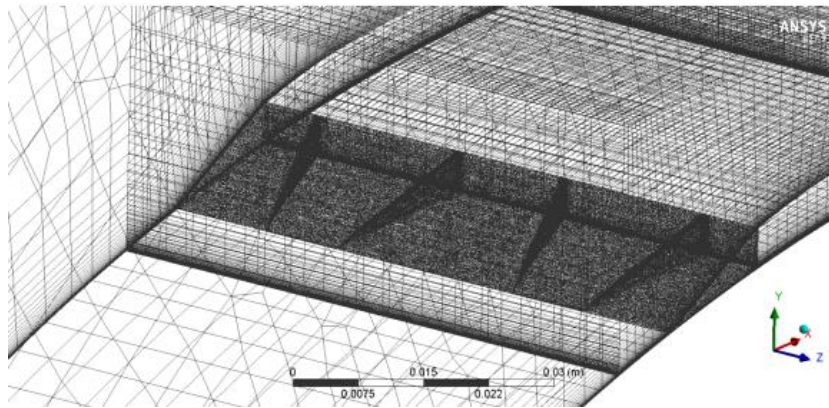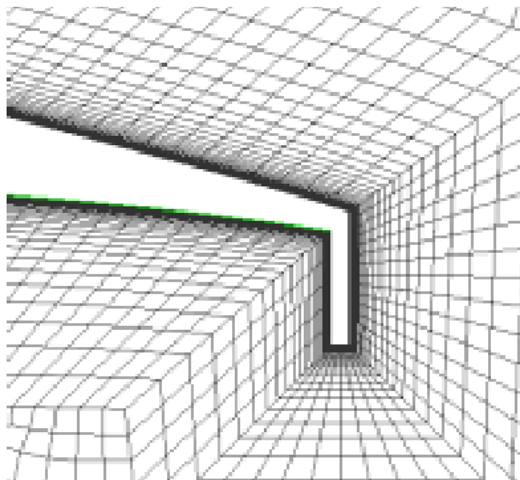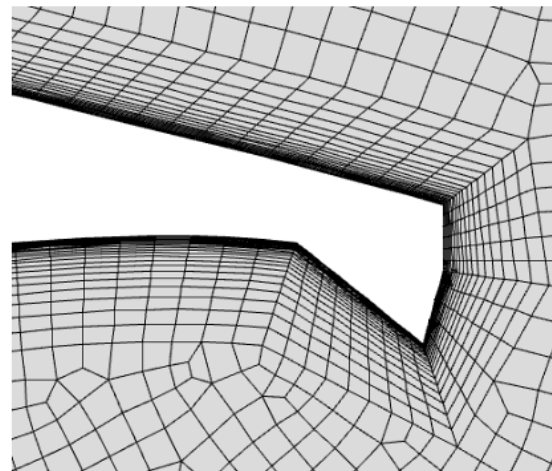
**Figure 5. The grid generated for the whole domain**



(a)



(a)                                                                (b)

**Figure 6. Nearfield pictures of grid in the regions of (a) vortex generators, (b) Gurney flap and (c) trailing-edge wedge**

To perform grid independent study, lift and drag coefficients of the airfoil equipped with VGs for three grid levels are obtained and compared. The first grid level has around 910,000 computational cells. The second and third grid levels are obtained by 30% increase in the computational cells relative to the prior grid level. So, the second and third grid levels have around 1,180,000 and 1,530,000 computational cells, respectively. Exploring the generated grids shows that for the three grid levels, maximum value of $y^+$ ($=y\sqrt{\tau/\rho}/\nu$, where $\tau$ stands for wall shear stress and $\nu$ is fluid kinematic viscosity) is around $y^+\approx1$. Figure 7 presents the obtained lift and drag coefficients of the airfoil for the three grid levels. Figures 8 and 9 also present the lift and drag coefficients of the airfoil equipped with VGs in the presence of Gurney flap and trailing-edge wedge with $H/c$=2% for the considered grid levels. These figures confirm that the second grid level has enough accuracy for numerical calculations.
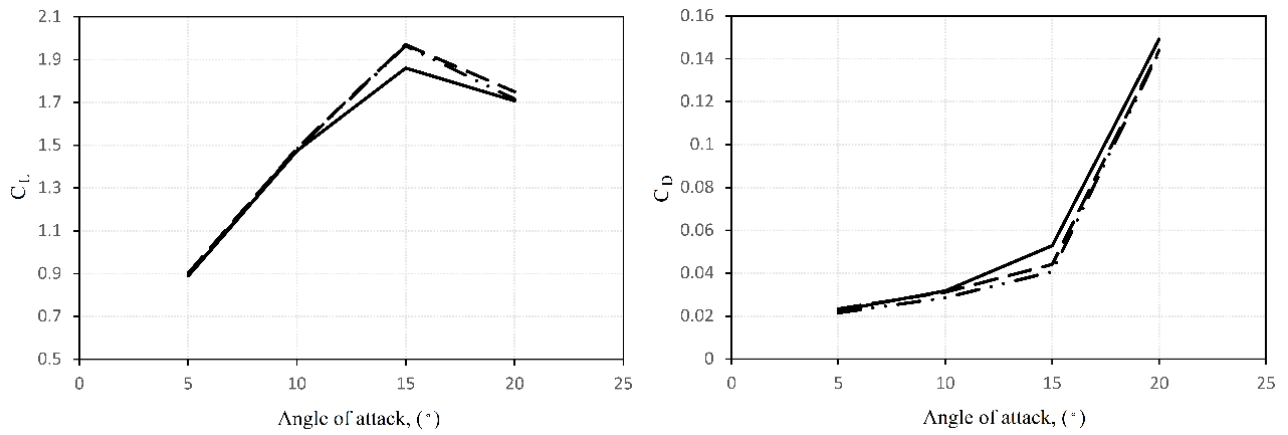
**Figure 7. Lift and drag coefficients of the airfoil equipped with VGs for the three grid levels. Grid level I (*solid*), Grid level II (*dashed*), Grid level III (*dashed dot dot*)**
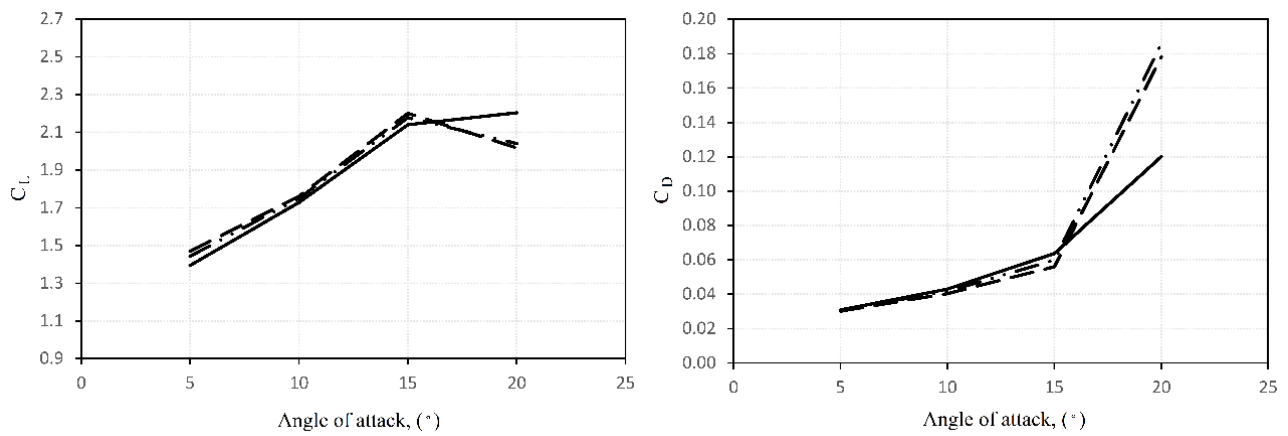


**Figure 8. Lift and drag coefficients of the airfoil equipped with VGs in the presence of Gurney flap with *H/c=2%* for the three grid levels. Grid level I (*solid*), Grid level II (*dashed*), Grid level III (*dashed dot dot*)**
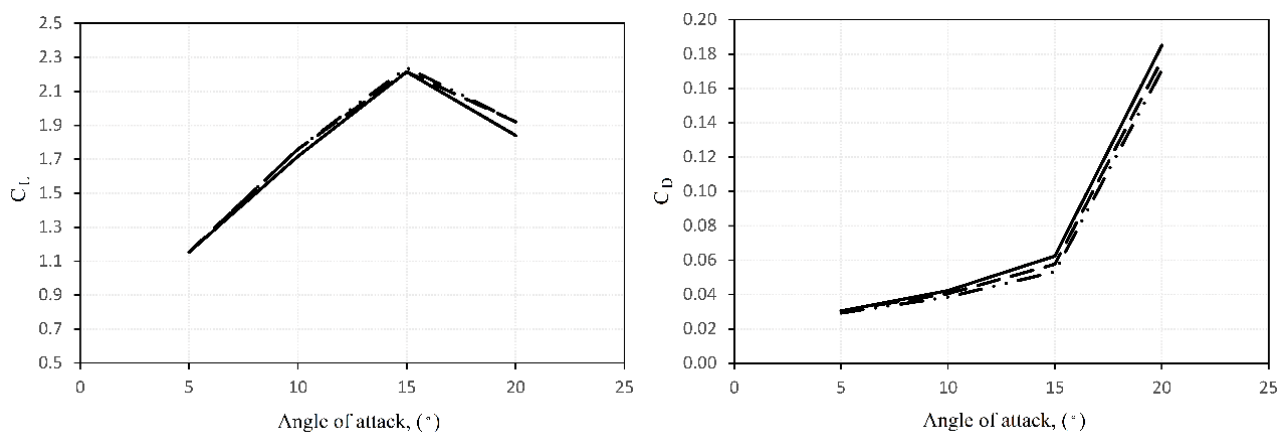


**Figure 9. Lift and drag coefficients of the airfoil equipped with VGs in the presence of trailing-edge wedge with *H/c=2%* for the three grid levels. Grid level I (*solid*), Grid level II (*dashed*), Grid level III (*dashed dot dot*)**

To validate the numerical model used for simulation of flow, aerodynamic coefficients of the airfoil equipped with VGs are compared with those of experiment. For more validation, comparison are also made for the clean airfoil (in the absence of vortex generators) in the presence of Gurney flap and trailing-edge wedge with those obtained from experiment. Figure 10 compares lift and drag coefficients of the airfoil equipped with VGs with those of the experiment [5] at Reynolds number of $3\times10^6$. This figure shows a good agreement between the current research and experiment.
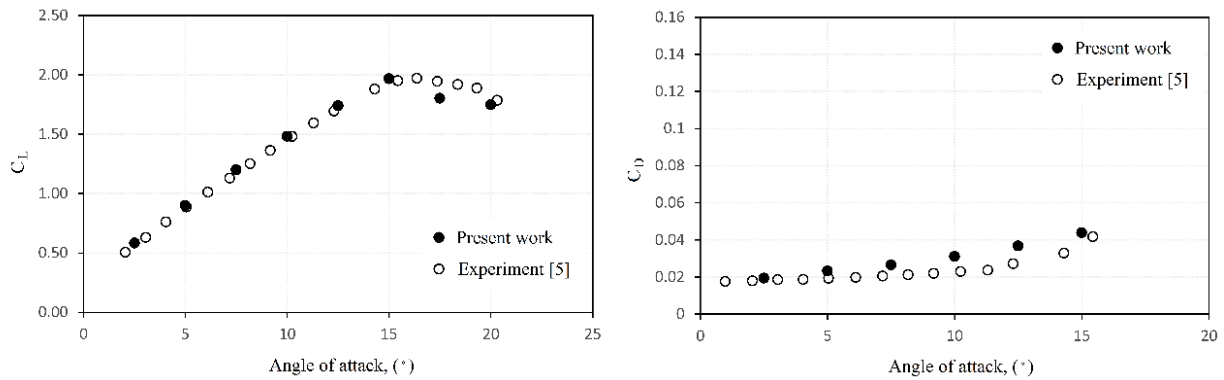
**Figure 10. Comparison of lift and drag coefficients of the airfoil equipped with VGs with those of the experiment**

Figure 11 shows lift coefficient of the clean airfoil in the presence of Gurney flap attained from the present work and experiment [5]. Consistent with experiment, results are obtained for the airfoil DU93-W-210 at Reynolds number of $2\times10^6$. As shown in Figure 11, there is a good concordance between the current research and experimental results.
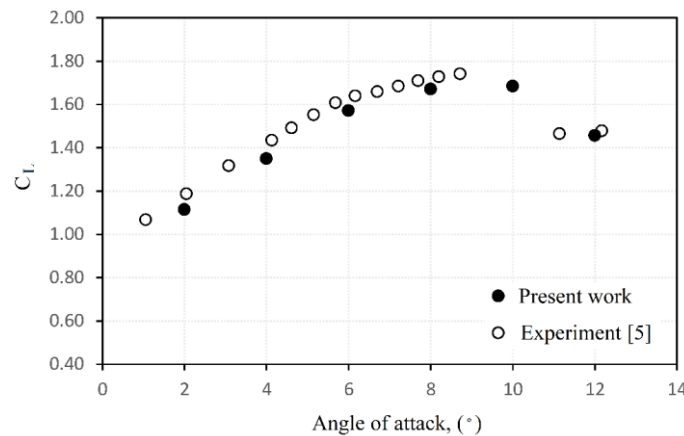


**Figure 11. Lift coefficient of the clean airfoil in the presence of Gurney flap attained form the present work and experiment**

Our numerical results also reveals that for the clean airfoil DU93-W-210 in the presence of trailing-edge wedge, the maximum lift to drag ratio at Reynolds number of $2\times10^6$ is 117.3. Referring to the work conducted by Timmer and Rooij [5], one could see that the maximum lift to drag ratio is reported to be 125.1, which is close to that of the present research.

# 5. Numerical Results and Discussion

## 5.1. Effect of Gurney Flap

Figure 12 presents lift coefficient, drag coefficient and aerodynamic performance of the airfoil equipped with VGs in the presence of Gurney flap at different Gurney flap heights. The abbreviations V.G and V.G+G.F stand for the equipped airfoil (clean airfoil in the presence of vortex generators) and the equipped airfoil in the presence of Gurney flap, respectively.
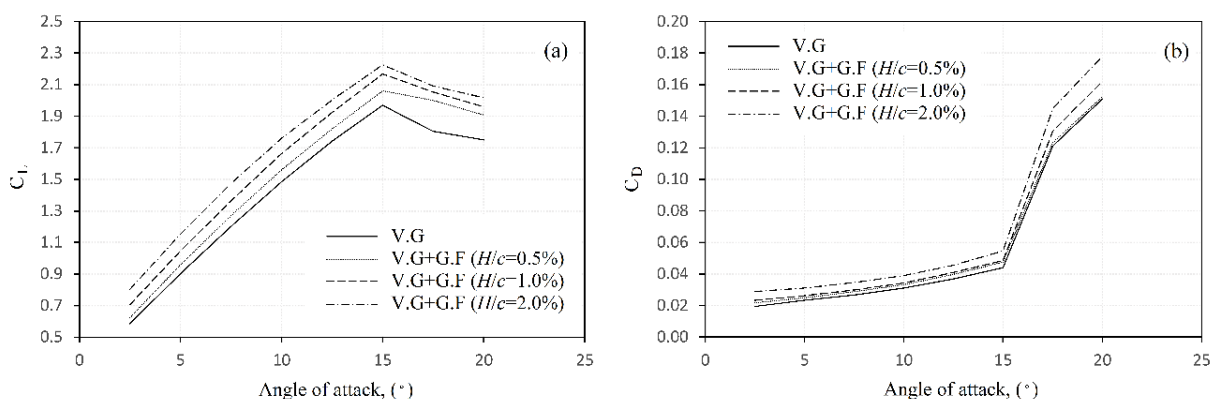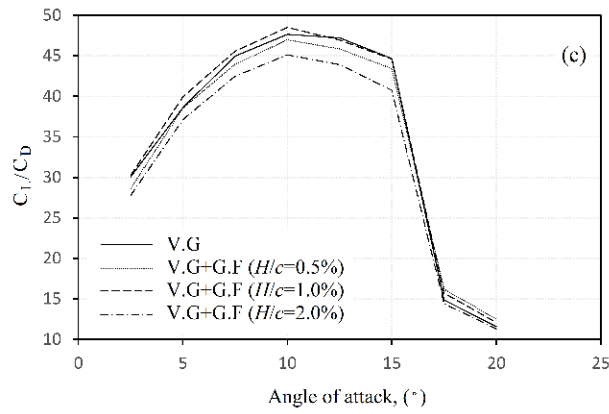
**Figure 12. Lift coefficient, drag coefficient and aerodynamic performance for the airfoil equipped with VGs in the presence of Gurney flap**

As Figures 12(a) and 12(b) represent, employment of Gurney flap leads to the increase in the airfoil lift and drag. These figures also reveal that the airfoil lift and drag increase as Gurney flap height increases. To explain more, flow structure at the middle plane for the equipped airfoil in the absence and presence of Gurney flap at different heights at stall angle of attack are presented in Figure 13. As this figure indicates, employment of Gurney flap leads to trapping the air ahead of Gurney flap and consequently generation of recirculation zone. This zone gets bigger as Gurney flap height increases. This phenomenon causes the pressure below the airfoil surface around the trailing edge and so the airfoil lift and drag to increase.
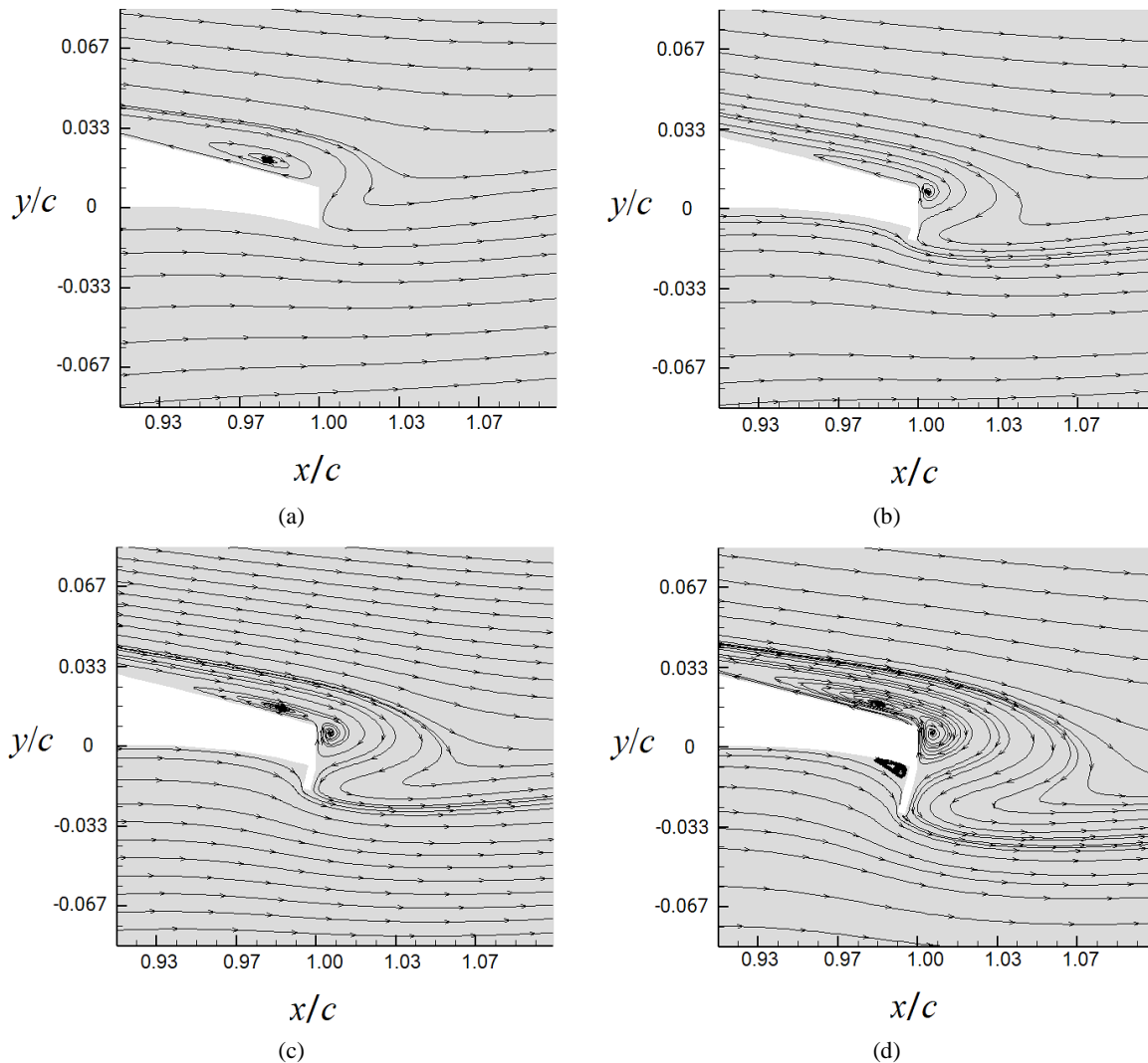


**Figure 13. Flow structure at the middle plane for the airfoil equipped with (a) VGs and for the airfoil equipped with VGs in the presence of Gurney flap at heights of  (b) $H/c$=0.5%, (c) 1% and (d) 2%**

Exploring Figure 12(a) shows that at stall angle of attack, the maximum lift increment which is associated to the Gurney flap height of $H/c$=2% is 13%. As Figure 12(c) represents, employment of Gurney flap with height ratio of $H/c$=1% could enhance the aerodynamic performance before stall. This means that the increase in the airfoil lift is superior to the increase in the airfoil drag before stall when Gurney flap with height ratio of $H/c$=1% is employed. Figure 12(c) also reveals that at stall region, the deterioration in aerodynamic performance associated to the Gurney flap height ratio of $H/c$=1% is minor compared to the other Gurney flap height ratios and aerodynamic performance of airfoil at this Gurney flap height ratio is nearly equal to that of the airfoil equipped with VGs. Results indicate that before stall, maximum increment attained for the aerodynamic performance which occurs at angle of 5 degrees is 3.4%.

## 5.2. Effect of Trailing-edge Wedge

Figure 14 shows lift coefficient, drag coefficient and aerodynamic performance of the airfoil equipped with VGs in the presence of trailing-edge wedge at different trailing-edge wedge heights. The abbreviation V.G+W is used for the airfoil equipped with VGs in the presence of trailing-edge wedge.
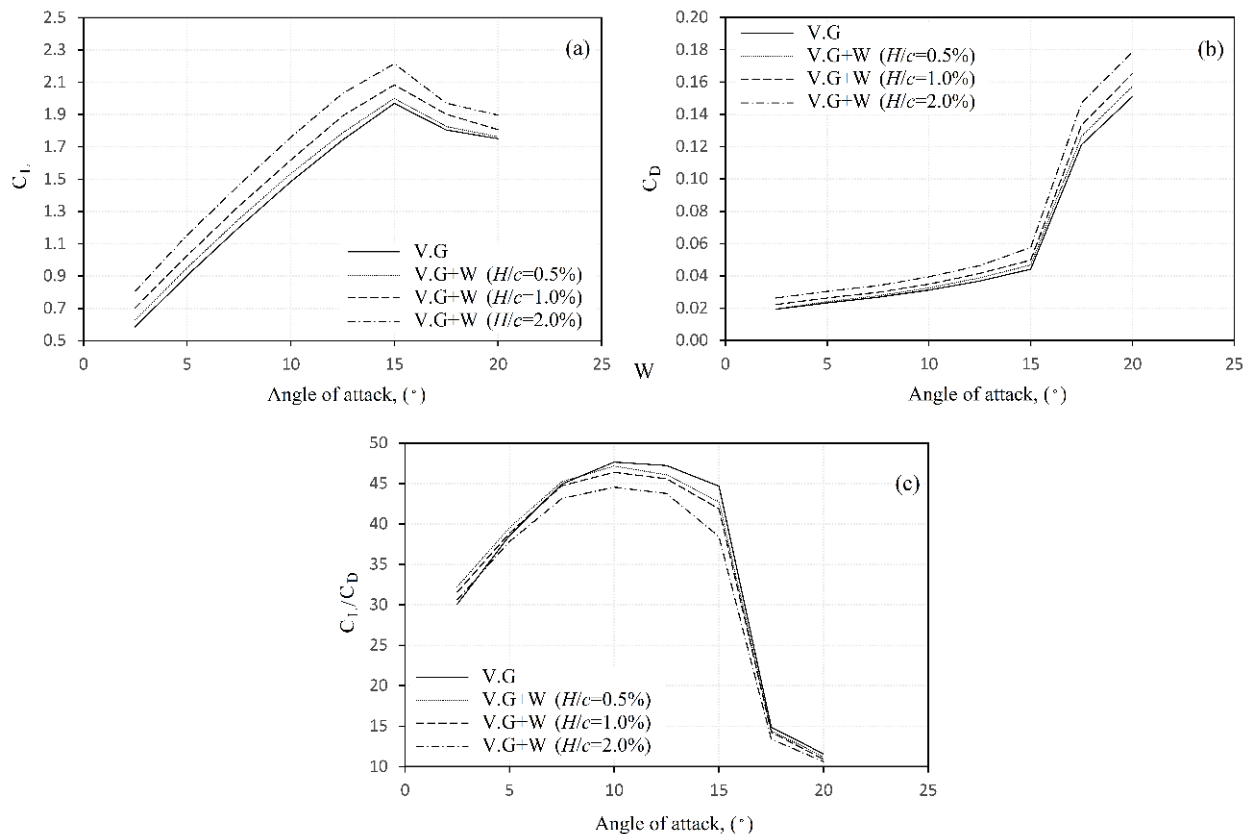


**Figure 14. Lift coefficient, drag coefficient and aerodynamic performance for the airfoil equipped with VGs in the presence of trailing-edge wedge**

As presented in Figures 14(a) and 14(b) represent, as expected, addition of trailing-edge wedge to the airfoil results in the increase in the airfoil lift and drag and the airfoil lift and drag increase as trailing-edge wedge height increases. For better understanding, streamlines at stall angle of attack in the middle plane for different wedge heights are presented in Figure 15. This figure reveals that the presence of trailing-edge wedge results in deflection of streamlines below the airfoil and this deflection increases as wedge heights increases. This means that the pressure below the airfoil increases as trailing-edge wedge is employed and this increment increases as wedge height increases. Thus, one could conclude that employment of trailing-edge wedge causes higher airfoil lift and drag and an increase in the wedge height leads to the increase in the airfoil lift and drag.
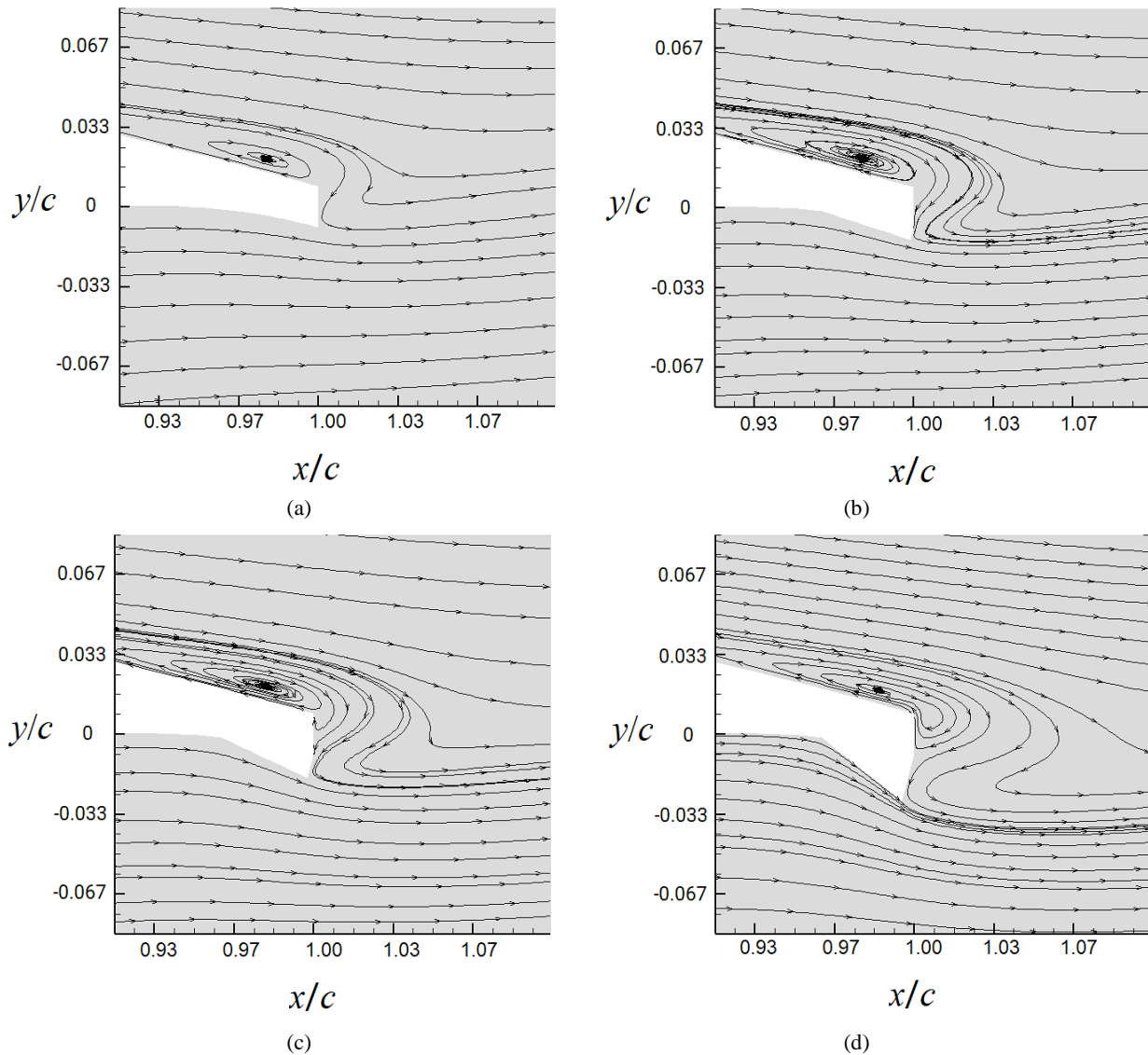
**Figure 15. Flow structure at the middle plane for the airfoil equipped with (a) VGs and for the airfoil equipped with VGs in the presence of trailing-edge wedge at heights of (b) *H/c*=0.5%, (c) 1% and (d) 2%**

Figure 14(a) exhibits that at stall angle of attack, maximum lift increment which corresponds to the wedge height of *H/c*=2% is 12.5%. As Figure 14(c) represents, employment of wedge could enhance the aerodynamic performance at low angles of attacks (below 5 degrees) and aerodynamic performance increases as wedge height decreases. This indicates that the increase in the airfoil lift is superior to the increase in the airfoil drag at low angles of attacks when trailing-edge wedge is employed. Numerical findings show that maximum increment for the aerodynamic performance which is associated to the wedge height of *H/c*=0.5% is 7.1% and appears at angle attack of 2.5 degrees.

As mentioned earlier, at stall angle of attack, the maximum lift increment for the airfoil equipped with VGs is 13% in the presence of Gurney flap while in the presence of trailing-edge wedge, the maximum lift increment is 12.5%. Since the lift increment for the airfoil is mainly due to increase in the pressure on the airfoil lower surface around the trailing edge, the pressure coefficient (i.e., $cp = (p - p_\infty)/\frac{1}{2}\rho V^2$, where $p$ and $p_\infty$ stand for the pressure on the airfoil surface and pressure in infinity, respectively) a stall angle of attack on the pressure side around the airfoil trailing edge for the airfoil equipped with VGs in the presence of Gurney flap and tailing-edge wedge are presented in Figure 16. This figure is provided for Gurney flap and wedge height of *H/c*=2%. As Figure 16 represents, employment of Gurney flap leads to a higher pressure on the airfoil lower surface than the trailing-edge wedge. This issue could also be confirmed by exploring Figures 13(d) and 15(d). Comparison of these figures reveals that, contrary to trailing-edge wedge, employment of Gurney flap results in trapping the air and generation of recirculation zone. This effect causes the Gurney flap to lead to a higher pressure below the airfoil surface than the wedge. Thus, as the lift is a strong function of pressure, higher lift increment is obtained when Gurney flap is used.
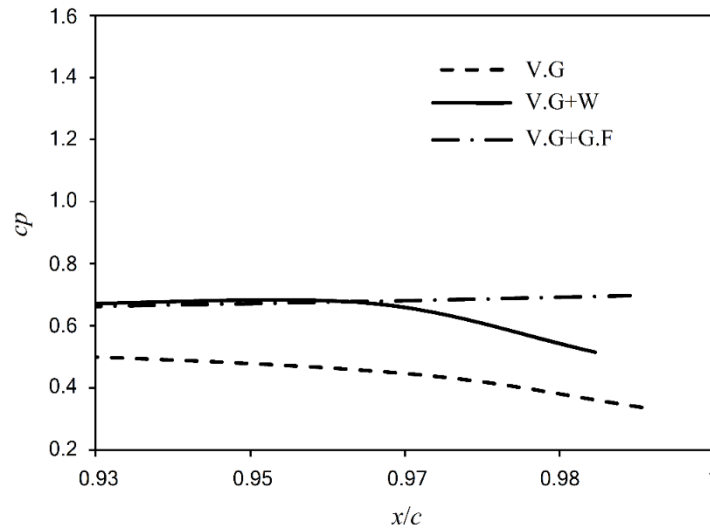
**Figure 16. Pressure coefficient a stall angle of attack on the pressure side around the airfoil trailing edge for the airfoil equipped with VGs in the presence of Gurney flap and tailing-edge wedge**

As one could see in Figure 12(c), employment of Gurney flap leads to improve in the aerodynamic performance below 12.5°. Exploring Figure 14(c) reveals that using trailing-edge wedge causes the aerodynamic performance to improve below around 7.5°. This means that before the stall, Gurney flap leads to improve in the aerodynamic performance in a wider range of angle of attack than the trailing-edge wedge.

For more illustration regarding the effect of Gurney flap and trailing-edge wedge on the aerodynamic behavior of the airfoil equipped with VGs, aerodynamic performance of the airfoil where the highest lift occurs are compared. Referring to Figures 12(a) and 14(a), one could see that Gurney flap and wedge with height of $H/c=2\%$ results in the highest value for the lift. So, for this Gurney and wedge heights, aerodynamic performance of the airfoil are presented and compared in Figure 17.
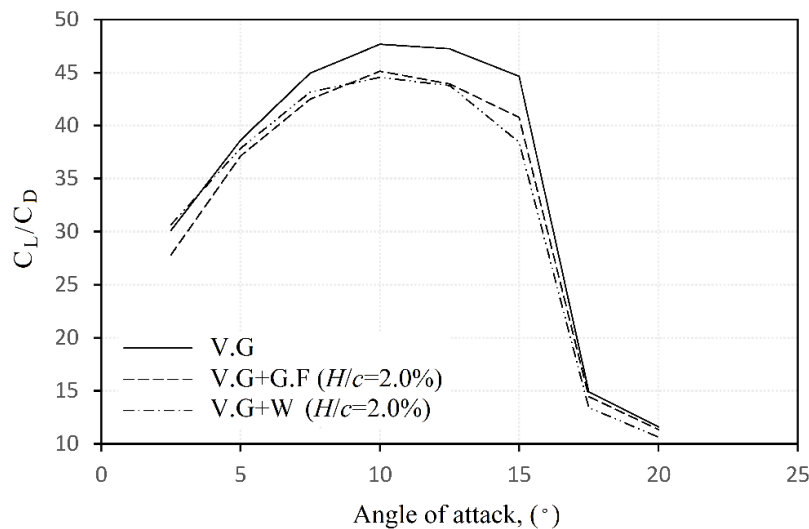


**Figure 17. Comparison of aerodynamic performance of the airfoil equipped with VGs in the presence of Gurney flap and trailing-edge wedge at height of $H/c=2\%$**

Figure 17 reveals that although employment of Gurney flap and trailing-edge wedge at height of $H/c=2\%$ causes the lift of the airfoil equipped with VGs to increase, however, addition of these high lift devices results in deterioration of the aerodynamic performance. This figure shows that at low angles of attack, employment of trailing-edge wedge leads to a better aerodynamic performance and at high angles of attack, the Gurney flap results in a better performance.

Referring to Figures 12(c), one could see that the Gurney flap at height of $H/c=1\%$ yields the highest airfoil performance before stall. Exploring Figure 14(c) shows that the trailing-edge wedge with height of $H/c=0.5\%$ and below around 7.5 degrees results in the highest performance. Comparison of Figure 12(a) with 14(a) reveals that, when high aerodynamic performance is concerned, addition of Gurney flap at height of $H/c=1\%$ to the airfoil equipped with VGs leads to the highest lift.

## 6. Conclusions

In the present work, the impact of the Gurney flap and trailing-edge wedge on the aerodynamics of the airfoil Du97-W-300 equipped with VGs is examined numerically. Various heights for the Gurney flap and trailing-edge wedge are considered. The appropriateness of the considered numerical model is confirmed by the comparison of the obtained lift and drag coefficients with those of the experimental work. The findings of the research undertaken are as follows:

- Employment of Gurney flap with height ratio of $H/c$=1% results in the highest value for the aerodynamic performance and the maximum increment for the aerodynamic performance is 3.4%. For trailing-edge wedges, the height ratio of $H/c$=0.5% leads to the highest aerodynamic performance, and the maximum increment for the aerodynamic performance is 7.1%.

- Before stall, the addition of Gurney flap to the airfoil equipped with VGs leads to the enhancement of the aerodynamic performance in a wider range of angle of attack while the enhancement in aerodynamic performance associated to the trailing-edge wedge occurs in a narrower range of angle of attack.

- At the highest value of lift, employment of the trailing-edge wedge results in a higher aerodynamic performance at low angles of attack, while at high angles of attack, better aerodynamic performance is observed when the Gurney flap is employed.

- Before stall, when high aerodynamic performance is desired, employment of Gurney flap with height ratio of $H/c$=1% is preferred as the highest value for the lift is obtained for the Gurney flap at this height ratio.

## 7. Declarations

### 7.1. Author Contributions

### 7.2. Data Availability Statement

The data presented in this study are available on request from the corresponding author.

### 7.3. Funding

### 7.4. Declaration of Competing Interest

The authors declare that they have no known competing financial interests or personal relationships that could have appeared to influence the work reported in this paper.

## 8. References

[1] Taylor, H. D. (1947). The elimination of diffuser separation by vortex generators. United Aircraft Corporation Report, R-4012-3(R4012-3), Moscow, Russia.

[2] Zhang, L., Li, X., Yang, K., & Xue, D. (2016). Effects of vortex generators on aerodynamic performance of thick wind turbine airfoils. Journal of Wind Engineering and Industrial Aerodynamics, 156, 84–92. doi:10.1016/j.jweia.2016.07.013.

[3] Zhu, C., Chen, J., Wu, J., & Wang, T. (2019). Dynamic stall control of the wind turbine airfoil via single-row and double-row passive vortex generators. Energy, 189, 116272. doi:10.1016/j.energy.2019.116272.

[4] Baldacchino, D., Ferreira, C., Tavernier, D. De, Timmer, W. A., & van Bussel, G. J. W. (2018). Experimental parameter study for passive vortex generators on a 30% thick airfoil. Wind Energy, 21(9), 745–765. doi:10.1002/we.2191.

[5] Timmer, W. A., & van Rooij, R. P. J. O. M. (2003). Summary of the Delft University wind turbine dedicated airfoils. 41st Aerospace Sciences Meeting and Exhibit, 125(4), 488–496. doi:10.2514/6.2003-352.

[6] Mueller-Vahl, H., Pechlivanoglou, G., Nayeri, C. N., & Paschereit, C. O. (2012). Vortex generators for wind turbine blades: A combined wind tunnel and wind turbine parametric study. Proceedings of the ASME Turbo Expo, 6, 899–914. doi:10.1115/GT2012-69197.

[7] Velte, C. M., & Hansen, M. O. L. (2013). Investigation of flow behind vortex generators by stereo particle image velocimetry on a thick airfoil near stall. Wind Energy, 16(5), 775–785. doi:10.1002/we.1541.

[8] Zhao, Z., Shen, W., Wang, R., Wang, T., Xu, B., Zheng, Y., & Qian, S. (2017). Modeling of wind turbine vortex generators in considering the inter-effects between arrays. Journal of Renewable and Sustainable Energy, 9(5), 53301. doi:10.1063/1.4997039.

[9] Prince, S. A., Badalamenti, C., & Regas, C. (2017). The application of passive air jet vortex-generators to stall suppression on wind turbine blades. Wind Energy, 20(1), 109–123. doi:10.1002/we.1994.

[10] Martinez Suarez, J., Flaszynski, P., & Doerffer, P. (2018). Application of rod vortex generators for flow separation reduction on wind turbine rotor. Wind Energy, 21(11), 1202–1215. doi:10.1002/we.2224.

[11] Zhu, C., Chen, J., Wu, J., & Wang, T. (2019). Dynamic stall control of the wind turbine airfoil via single-row and double-row passive vortex generators. Energy, 189, 116272. doi:10.1016/j.energy.2019.116272.

[12] Nikoueeyan, P., Strike, J. A., Magstadt, A. S., Hind, M. D., & Naughton, J. W. (2014). Characterization of the static aerodynamic coefficients of a wind turbine airfoil with gurney flap deployment for flow control applications. 32nd AIAA Applied Aerodynamics Conference, 16–20. doi:10.2514/6.2014-2146.

[13] Alber, J., Pechlivanoglou, G., Paschereit, C. O., Twele, J., & Weinzierl, G. (2017). Parametric investigation of gurney flaps for the use on wind turbine blades. Proceedings of the ASME Turbo Expo, 9. doi:10.1115/GT2017-64475.

[14] Zhang, Y., Ramdoss, V., Saleem, Z., Wang, X., Schepers, G., & Ferreira, C. (2019). Effects of root Gurney flaps on the aerodynamic performance of a horizontal axis wind turbine. Energy, 187, 115955. doi:10.1016/j.energy.2019.115955.

[15] Gao, L., Liu, Y., Han, S., & Yan, J. (2014). Aerodynamic performance of a blunt trailing-edge airfoil affected by vortex generators and a trailing-edge wedge. IET Conference Publications, 2014(CP651), 24–25. doi:10.1049/cp.2014.0917.

[16] Yan, P., Han, S., Liu, Y., Gao, L., & Li, L. (2015). Effects of gurney flap and trailing-edge wedge on a blunt trailing-edge aerofoil. IET Conference Publications, 2015(CP679), 17–18,. doi:10.1049/cp.2015.0484.

[17] Gao, L., Zhang, H., Liu, Y., & Han, S. (2015). Effects of vortex generators on a blunt trailing-edge airfoil for wind turbines. Renewable Energy, 76, 303–311. doi:10.1016/j.renene.2014.11.043.

[18] Agarwal, R., Dhamarla, A., Narayanan, S. R., Goswami, S. N., & Srinivasan, B. (2014). Numerical Investigation on the Effect of Vortex Generator on Axial Compressor Performance. Volume 2A: Turbomachinery. doi:10.1115/gt2014-25329.

[19] Godard, G., & Stanislas, M. (2006). Control of a decelerating boundary layer. Part 1: Optimization of passive vortex generators. Aerospace Science and Technology, 10(3), 181–191. doi:10.1016/j.ast.2005.11.007.

[20] Snel, H. (2003). Review of aerodynamics for wind turbines. Wind Energy, 6(3), 203–211. doi:10.1002/we.97.

[21] Bai, C. J., Hsiao, F. B., Li, M. H., Huang, G. Y., & Chen, Y. J. (2013). Design of 10 kW horizontal-axis wind turbine (HAWT) blade and aerodynamic investigation using numerical simulation. Procedia Engineering, 67, 279–287. doi:10.1016/j.proeng.2013.12.027.